Single-Frequency Q-Switched Cr–Nd:YAG Laser Operating at 946-nm Wavelength

Hua Liu, Osmany Hornia, Y. C. Chen, and Shou-Huan Zhou

***Abstract*— Single-frequency *Q*-switched operation in 946-nm wavelength has been demonstrated by application of a monolithic Cr–Nd:YAG cavity. In this device, the Cr–Nd:YAG laser material performs the functions of light modulation, frequency stabilization, and polarization selection. The conditions for the single-frequency operation and maximum degree of polarization are discussed.**

***Index Terms*— Passive *Q*-switching, *Q*-switching, single frequency.**

Q-SWITCHED lasers are widely used in applications such as laser remote sensing, laser satellite networking, laser communication, and many nonlinear optical experiments. Most of the applications require additional properties of the Q-switched lasers, such as single longitudinal mode, single transverse mode, stable pulse shape and pulsewidth, or ultra-compact and rugged oscillators with some, or all, of the above properties. In principle, these additional requirements can be satisfied by adding intra-cavity components to perform light modulation, frequency selection, polarization selection, and transverse-mode control. Each additional component invariably causes additional system complexity and instability.

A simpler approach would be to use a multifunctioned laser material to perform the functions that are normally done by the conventional laser cavity. An example of this multifunctioned material is the Cr and Nd codoped host crystals in which the tetravalent Cr ions behave as the saturable absorber for inducing Q-switching at 1064 nm [1]–[5]. The distributed saturable absorber also stabilizes the longitudinal mode through the self-induced loss granting [3], provides transverse-mode control through the aperture guiding [5], and defines the angle of polarization through the polarization-dependent saturation power [4], [6]. Indeed, the monolithic Cr–Nd:YAG lasers have been demonstrated to generate Q-switched pulses in single longitudinal mode and single transverse mode with a high degree of polarization at 1064-nm wavelength [3], [4]. Passively Q-switched microchip lasers based on solid-state saturable absorbers have also been demonstrated by Braun *et al.* [6] and Zayhowski *et al.* [8].

Manuscript received December 2, 1996; revised January 15, 1997. This work was supported by the Ballistic Missile Defense Organization under Grant N00014-96-1-5018, Quantum Electronics Technology, Inc., the New York State Center for Advanced Technology (CAT) on Ultrafast Photonic Materials and Applications at the City University of New York, and the NASA Institutional Research Award.

H. Liu, O. Hornia, and Y. C. Chen are with the New York State Center for Advanced Technology on Ultrafast Photonic Materials and Applications, Department of Physics and Astronomy, City University of New York (CUNY), Hunter College, New York, NY 10021 USA.

S.-H. Zhou is with the North China Research Institute of Electro-Optics, Beijing, P.R. China.

Publisher Item Identifier S 1077-260X(97)03765-9.

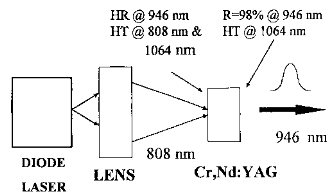

Fig. 1. Schematic of the experimental setup.

In this paper, we report the operation of a diode-pumped monolithic Q-switched Cr–Nd:YAG laser emitting at 946-nm wavelength. The 946-nm laser has attracted considerable interest for the usefulness of its blue–green second-harmonic emission in underwater imaging and communication applications [9]–[12]. Previously, Fan *et al.* [9] have done extensive study on the quasi-three-level 946-nm Nd:YAG lasers. Room-temperature continuous-wave (CW) operation in single frequency by injection locking [10], by application of a composite-cavity nonplanar ring cavity [11], and by resonant excitation [12] have also been reported. The effect of aperture-guiding in a three-level laser has also been studied [5]. The broad-band saturable absorption of Cr^{4+} in YAG covers a wide spectral range from 900 to 1200 nm [2], [13]. It is of interest to investigate the single-frequency Q-switched operation at 946 nm using a much simpler monolithic cavity.

The schematic of the experimental setup is shown in Fig. 1. The output of a 2-W diode laser emitting at 808-nm wavelength is imaged onto the Cr–Nd:YAG rod and is absorbed in a single pass. The Cr–Nd:YAG crystal contains 1-wt% Nd. The absorption coefficient of Cr^{4+} at 946 nm is 0.15 cm^{-1}. To reduce the effect of the ground-state absorption caused by the thermally populated lower state of the laser transition in the $^4I_{9/2}$ manifold, the length of the crystal is chosen to be 3 mm. The laser crystal is polished to form a flat–flat Fabry–Perot cavity. The mirror facing the pump beam is coated for $>$80% transmission at both 808 and 1064 nm, and $>$99.5% reflection at 946 nm. The output mirror is coated for 98% reflectivity at 946 nm and $>$50% transmission at 1064 nm.

The lasing threshold is reached at a pump power of 1 W under CW pumping. The output power versus pump energy characteristics is shown in Fig. 2. Above the threshold, the slop efficiency of energy conversion is 12%. The output consists of a train of Q-switched pulses. The pulse duration is 4.6 ns. The repetition frequency is 3.5 kHz when the output power is 25 mW, corresponding to a pulse energy of 7 μJ per pulse. As

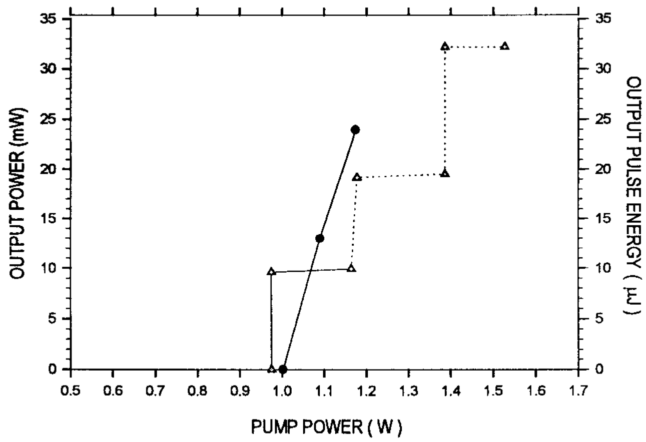

Fig. 2. CW output power (circles) and quasi-CW pulse energy (triangles) versus pump-power characteristics of a monolithic Q-switched Cr–Nd:YAG laser operating at 946 nm. The single-frequency (solid lines) and two-frequency (dotted lines) regions are indicated. The triangles are experimental points.

the pump power increases, the repetition rate increases, while the pulse energy and pulse duration remain nearly constant.

The smallest spot size of the pump beam in the laser crystal is approximately 100 μm (vertical) $\times$ 150 μm (horizontal). A close examination of the cross section of the pump beam in the laser crystal using a video camera reveals that the size of the excited region in the vertical direction remains nearly constant throughout the cavity, while the size in the horizontal direction varies from 150 μm at the input end to 300 μm at the opposite end of the 3-mm-long cavity. Despite the rectangular-shaped excited region, the laser oscillating mode is nearly circular with a full-width-at-half-maximum (FWHM) beam diameter of 150 μm. The laser operates in a Gaussian-like TEM_{00} mode at all pump powers.

The experimentally measured degree of polarization varies from 0 to 1, corresponding to linearly polarized light, as the Cr–Nd:YAG crystal is rotated about the [100] axis. For a given crystal orientation, the polarization does not change from pulse to pulse. When the degree of polarization is 1, the electric field is parallel to the junction plane of the diode laser. We have also observed that the highest degree of polarization also corresponds to the lowest lasing threshold. This phenomenon suggests that the laser cavity contains two polarization-defining mechanisms. One of the mechanisms already known to us is the anisotropy in the saturation power of the Cr^{4+} absorption reported by Eilers *et al.* [6]. The absorption coefficient of Cr:YAG at 1064-nm wavelength is isotropic at low powers and becomes anisotropic with a fourfold symmetry about the [100] axis at high powers. This effect promotes a linearly polarized lasing mode whose electric field is parallel to the direction of minimum saturation power. There exists a second mechanism of unknown nature, whose preferred axis is parallel to the junction plane of the diode lasers. When the axes of the two polarization-defining mechanisms coincide, the laser output has the highest degree of polarization.

We have estimated the magnitude of birefringence caused by the rectangular-shaped excited region. The absorption coefficient of the saturable absorption is 0.15 cm^{-1}, which corresponds to an imaginary refractive index of 1×10^{-6}. When the laser reached the threshold, the refractive-index step between the bleached and unbleached regions creates a waveguide. A computer simulation for a rectangular-shaped gain–loss waveguide with a cross section of 100 μm $\times$ 200 μm and an index step of 1×10^{-6} reveals that the modal indices of the TE and TM modes differ by 1×10^{-10}, which is too small to cause any polarization rotation during a nanosecond pulse. The nature of the second polarization-defining mechanism is still being investigated.

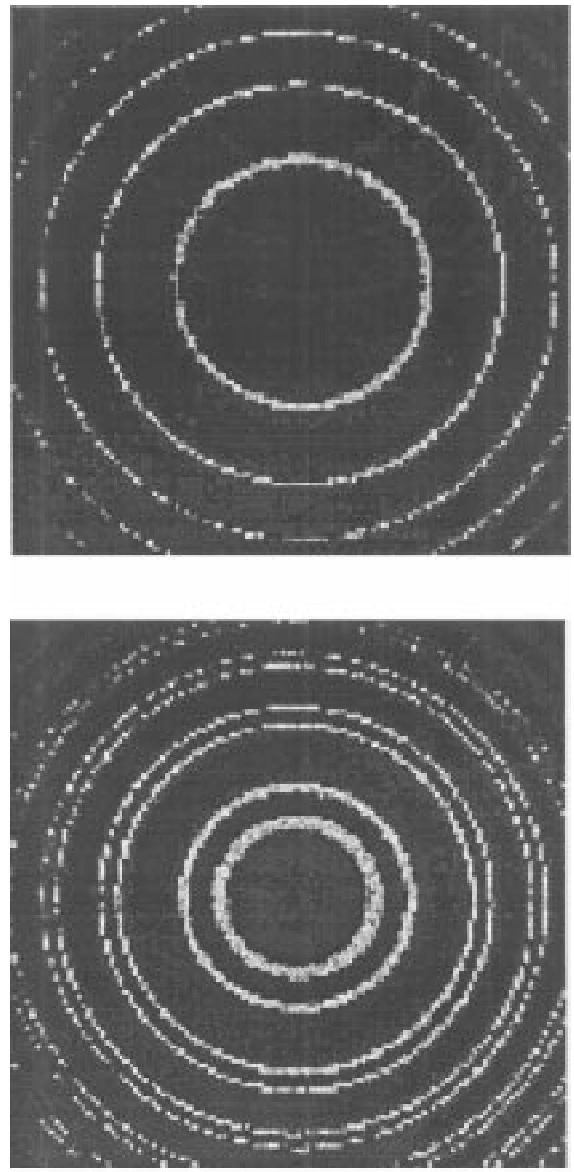

Fig. 3. Interferograms of single-frequency (upper) and two-frequency (lower) lasing spectra.

The lasing spectrum is monitored using a 5-mm-thick glass etalon with a finesse of 60. When the laser is pumped by a CW diode laser, the Q-switched laser output consistently operates in a single longitudinal mode, without pulse-to-pulse mode hopping for pump powers up to 20% above the threshold. Without any active temperature regulation for the laser rod, the frequency shift at room temperature is less than 1 GHz over a 1-min period. A single-frequency interferogram recorded using a charge-coupled device (CCD) camera is shown in Fig. 3. The single-frequency operation is attributed to the self-induced frequency-stabilization effect caused by the loss grating in the cavity, which is established in the Cr–Nd:YAG crystal when the lasing mode bleaches the saturable absorber [3]. The grating creates a low-loss window centered at the frequency of the lasing mode. In the absence of the loss grating, the Nd:YAG lasers would normally operate in multiple longitudinal modes due to the spatial-hole-burning effect in the gain medium. The loss granting offsets the spatial-hole-burning effect and stabilizes the central lasing mode within the gain bandwidth. When the laser is operated in the single-frequency regime, the pulse-to-pulse intensity fluctuation is less than 1%, which is the resolution limit of our instrument.

Since the Q-switched pulse energy remains nearly constant as the pump power increases, the modulation depth of the loss grating is independent of pump power while the gain of the nonlasing mode increases with pump power. At a higher pump power, the loss grating can no longer stabilize the central lasing mode. In the present experiment, the onset of multimode emission occurs when the pump power exceeds 1.2 W. An interferogram of a two-mode lasing spectrum is shown in Fig. 3. The onset of the multimode operation is also accompanied by increased pulse-to-pulse intensity fluctuation of about 5%.

Under quasi-CW pumping with 500-μs pulse duration at 100-Hz repetition rate, the lasing threshold is 0.97 W. The output pulse energy versus pump-power characteristics are shown in Fig. 2. The step-like relation at higher pump power is due to the occurrence of multiple pulses during a single pump pulse. We have found that the Q-switched laser always operates in a single frequency as long as the pulse duration and pump power are adjusted so that each pump pulse generates only one Q-switched pulse. The regimes of single-frequency operation are marked by solid lines in Fig. 2. When the laser is pumped by a quasi-CW diode-laser pulse, the time separation between the pump pulses is longer than the lifetime of the excited state of the laser transition. Thus, terminating the pump pulse after each Q-switched pulse and allowing enough time for the spatial holes in the gain medium to dissipate, is an effective way of ensuring the single-frequency operation.

In summary, a monolithic Cr–Nd:YAG laser has been demonstrated to emit Q-switched laser pulses in single frequency with a high degree of polarization at 946-nm wavelength. In this device, the Cr–Nd:YAG performs the functions of light modulation, frequency stabilization, and polarization selection. The conditions for single-frequency operation and a maximum degree of polarization are also discussed.

References

[1] A. A. Danilov, E. V. Zharikov, A. I. Zagumennyi, G. B. Lutts, and M. Y. Nikol'skii, "Self-Q-switched high-power laser utilizing gadolinium scandium aluminum garnet activated with chromium and neodymium," *Sov. J. Quantum Electron.*, vol 19, pp. 315–331, Apr. 1989.

[2] S. Li, S. Zhou, P. Wang, and Y. C. Chen, "Self-Q-switched Cr–Nd:YAG laser," *Opt. Lett.*, vol 18, pp. 203–205, Feb. 1993.

[3] Y. C. Chen, S. Li, K. K. Lee, and S. Zhou, "Self-stabilized single longitudinal mode operation in self-Q-switched solid-state lasers," *Opt. Lett.*, vol 18, pp. 1418–1420, Sept. 1993.

[4] S. Zhou, K. K. Lee, Y. C. Chen, and S. Li, "Monolithic self-Q-switched Cr–Nd:YAG laser," *Opt. Lett.*, vol 18, pp. 511–513, Apr. 1993.

[5] T. Y. Fan, "Aperture guiding in quasi-three-level lasers," *Opt. Lett.*, vol 19, pp. 554–556, Apr. 1994.

[6] H. Eilers, K. R. Hoffman, W. M. Dennis, S. M. Jacobson, and W. M. Yen, "Saturation of 1.064-μm absorption in Cr–Ca:YAG crystals," *Appl. Phys. Lett.*, vol 61, pp. 2958–2960, Dec. 1992.

[7] B. Braun, F. X. Kartner, U. Keller, J. P. Meyn, and G. Huber, "Passively Q-switched 180-ps $Nd:LaSc_3(BO_3)_4$ microchip laser," *Opt. Lett.*, vol 21, pp. 405–407, Mar. 1996.

[8] J. J. Zayhowski and C. Dill, III, "Diode-pumped passively Q-switched picosecond microchip lasers," *Opt. Lett.*, vol 19, pp. 1427–1429, Sept. 1994.

[9] T. Y. Fan and R. L. Byer, "Modeling and CW operation of a quasi-three-level 946-nm Nd:YAG laser," *IEEE J. Quantum Electron.*, vol QE-23, pp. 605–612, May 1985.

[10] G. Hollenmann, E. Peik, A. Rusch, and H. Walther, "Injection locking of a diode-pumped Nd:YAG laser at 946 nm," *Opt. Lett.*, vol 20, pp. 1871–1873, Sept. 1995.

[11] I. Freitag, R. Henking, A. Tunnermann, and H. Welling, "Quasi-three-level room-temperature Nd:YAG ring laser with single-frequency output power at 946 nm," *Opt. Lett.*, vol 20, p. 2499, Dec. 1995.

[12] J. P. Cuthbertson and G. J. Dixon, "Pump-resonant excitation of the 946-nm Nd:YAG laser," *Opt. Lett.*, vol 16, pp. 396–398, Mar. 1991.

[13] J. J. Miller, "Experimental investigation of Cr^{4+} in YAG as a passive Q-switch," in *OSA Proc. Advanced Solid-State Lasers*, Washington, DC, Feb. 1992, vol 12, pp. 322–325.

Hua Liu, photograph and biography not available at the time of publication.

Osmany Hornia, photograph and biography not available at the time of publication.

Y. C. Chen, photograph and biography not available at the time of publication.

Shou-Huan Zhou, photograph and biography not available at the time of publication.